Influence of γ-Fe_2O_3 nanoparticles doping on the image sticking in VAN-LCD

Ningning Liu (刘宁宁)[1], **Mohan Wang** (王墨涵)[1], **Zongyuan Tang** (唐宗元)[1], **Lin Gao** (高 林)[1], **Shuai Jing** (景 帅)[1], **Na Gao** (高 娜)[1], **Hongyu Xing** (邢红玉)[1,**], **Xiangshen Meng** (孟祥申)[2], **Zhenghong He** (何正红)[2], **Jian Li** (李 建)[2], **Minglei Cai** (蔡明雷)[3,4], **Xiaoyan Wang** (王晓燕)[3,4], **and Wenjiang Ye** (叶文江)[1,*]

[1]*School of Sciences, Hebei University of Technology, Tianjin 300401, China*
[2]*School of Physical Science and Technology, Southwest University, Chongqing 400715, China*
[3]*Hebei Jiya Electronics Co., Ltd., Shijiazhuang 050071, China*
[4]*Hebei Provincial Research Center of LCD Engineering Technology, Shijiazhuang 050071, China*
**Corresponding author: wenjiang_ye@hebut.edu.cn; **corresponding author: hongyu_xing@163.com*
Received October 23, 2019; accepted December 11, 2019; posted online March 9, 2020

Image sticking in liquid crystal display (LCD) is related to the residual direct current (DC) voltage (RDCV) on the cell and the dynamic response of the liquid crystal materials. According to the capacitance change of the liquid crystal cell under the DC bias, the saturated RDCV (SRDCV) can be obtained. The response time can be obtained by testing the optical dynamic response of the liquid crystal cell, thereby evaluating the image sticking problem. Based on this, the image sticking of vertical aligned nematic (VAN) LCD (VAN-LCD) with different cell thicknesses (3.8 μm and 11.5 μm) and different concentrations of γ-Fe_2O_3 nanoparticles (0.017 wt.%, 0.034 wt.%, 0.051 wt.%, 0.068 wt.%, 0.136 wt.%, 0.204 wt.%, and 0.272 wt.%) was evaluated, and the effect of nano-doping was analyzed. It is found that the SRDCV and response time decrease firstly and then increase with the increase of the doping concentration of γ-Fe_2O_3 nanoparticles in the VAN cell. When the doping concentration is 0.034 wt.%, the γ-Fe_2O_3 nanoparticles can adsorb most of the free impurity ions in liquid crystal materials, resulting in 70% reduction in the SRDCV, 8.11% decrease in the decay time, and 15.49% reduction in the rise time. The results show that the doping of γ-Fe_2O_3 nanoparticles can effectively improve the image sticking of VAN-LCD and provide useful guidance for improving the display quality.

Keywords: nanoparticles doping; image sticking; SRDCV; response time; VAN-LCD.
doi: 10.3788/COL202018.033501.

Liquid crystal display (LCD) devices are one of the most popular flat panel displays, which have many excellent characteristics, such as high resolution, small size, light weight, and low power consumption[1]. They are widely used in mobile phones, computers, televisions[2], public information display[3], and holographic projection display technology[4,5]. Among them, the vertical aligned nematic (VAN) LCD (VAN-LCD) has good dark state effect and can provide excellent contrast. It is widely used in transmission and reflective projection displays[6,7]. However, with the increasing demand for high-definition and fast display pictures, LCD panel production companies and researchers are working hard to improve the performance of LCDs. Image sticking is a key problem to improve the quality of LCDs. When the display screen displays a fixed picture for a long time and switches to the second display picture, the second picture and the weak image (image sticking) of the first picture will appear on the screen at the same time, which will affect the display effect of the second display picture[8–10]. It is well known that the main reasons for image sticking are the impure ions in the display screen and the direct current (DC) bias (DCB) in the driving circuit. When the two reasons exist at the same time[11,12], the electric field separates the positive and negative ions, forming the internal electric field, and the effective voltage on the liquid crystal (LC) decreases, which leads to the problem of image sticking.

The most primitive evaluation method of image sticking is human eye detection, which cannot make the evaluation results clearly at a glance[13]. Later, the optical minimum flicker method[14–17] and the electrical ion adsorption and desorption model method[18–20] became the main ways to evaluate the image sticking problem, but the minimum flicker method is vulnerable to the influence of environmental light, and the accuracy of the measurement results is low. The ion model method needs to determine a plurality of complex parameters when establishing a multi-ion model, so that the workload is increased. In 2018, Gao *et al.*[21] proposed a capacitance voltage method to evaluate image sticking and obtained residual DC voltage (RDCV) by measuring capacitance changes under alternating current (AC) and DCB, which is a simple and reliable electrical method. In order to overcome the image sticking problem of LCD, researchers have proposed a lot of improvement methods. Tsutsui *et al.*[22] and Seen *et al.*[23] studied the improvement of image sticking in in-plane switching (IPS) and fringe field switching (FFS) LCD modes by changing the aligned materials. Ye and Gao *et al.*[21,24] studied the improvement of image sticking in the parallel aligned nematic (PAN) LCD

mode by doping γ-Fe_2O_3 nanoparticles in LC materials with positive dielectric anisotropy. For the VAN display mode, image sticking can be improved by preparing a mixed monomer polymer layer[25,26]. However, when the monomer polymerization constant is small, the monomer may remain in the LC layer, resulting in a large RDCV. Nowadays, nanotechnology has penetrated into many fields[27], and its introduction into LCD can also effectively increase the display performance[28–30]. However, whether the mixture of LC with negative dielectric anisotropy with more impurity ions and γ-Fe_2O_3 nanoparticles can improve the image sticking in VAN cells needs to be further studied. For writing convenience, the LC with negative dielectric anisotropy was simplified as negative LC in the following description.

In this Letter, the RDCV and response time are analyzed by testing the curve of capacitance variation of the VAN LC cell under the simultaneous action of an AC and DCB and the curve of transmittance of the VAN LC cell with time under the action of AC; then, image sticking of VAN-LCD is evaluated. At the same time, the saturated RDCV (SRDCV) and response time of two kinds of VAN cells with different thickness of γ-Fe_2O_3 nanoparticles doping negative LC FFS1 were measured experimentally. The effect of nano-doping on VAN-LCD display image sticking was analyzed, and the optimum doping concentration was obtained, which is expected to be helpful for solving the image sticking problem of VAN-LCD.

The LC material used in this Letter is provided by Shijiazhuang Chengzhi Yonghua Display Materials Co., Ltd., and the type is FFS1, which is a negative LC. γ-Fe_2O_3 nanoparticles were obtained by chemical induced transformation[31–33] and wrapped in oleic acid. The average sizes of the coated composite nanoparticles (γ-Fe_2O_3/oleic acid) core and oleic acid were 10 nm and 2 nm, respectively. In order to obtain a uniform and non-precipitated nanoparticles LC mixture, a small amount of γ-Fe_2O_3 nanoparticles were added to *n*-hexane, sonicated for 40 min, and centrifuged at 5000 r/min for 30 min to obtain an *n*-hexane-based magnetic liquid. Take an equal amount of *n*-hexane and FFS1 LC and homogenize them ultrasonically; then take a small amount of *n*-hexane-based magnetic liquid, heat it to about 10°C above the clearing point of FFS1 LC, and shake it with a shaker until the *n*-hexane evaporates completely, thus obtaining the mixture of γ-Fe_2O_3 nanoparticles and FFS1 LC.

The LC mixture was poured into the PAN cell, and the temperature was controlled by precision hot stage LTS350 (Linkam, Surrey, UK) with an accuracy of ±0.1°C. When the LC changed from a liquid state to an LC state, the process of non-orientation to orientation of the molecule was observed under the polarizing microscope (POM) BX51 (Olympus, Tokyo, Japan), and the clearing point temperature of the LC mixture was obtained. The parallel dielectric constant $\varepsilon_{//}$ and vertical dielectric constant $\varepsilon_{\perp}$ of the LC mixture at 28°C were measured by the dual-cell capacitance model. The $\varepsilon_{//}$ can be obtained by the capacitance of the LC layer of the VAN cell when the voltage is lower than the threshold voltage, and the $\varepsilon_{\perp}$ can be obtained by the capacitance of the LC layer of the PAN cell when the voltage is higher than the threshold voltage. The LC molecule in the VAN cell shows only bending deformation after the electric field is applied. The k_{33} value of the LC mixture can be calculated by $(U_{\mathrm{th}})_{\mathrm{VAN}} = \pi^2\sqrt{k_{33}/\Delta\varepsilon\varepsilon_0}$, and the rotational viscosity coefficient γ_1 can be obtained by the response time $(\tau_{\mathrm{decay}})_{\mathrm{VAN}} = d^2\gamma_1/(\pi^2 k_{33})$[34].

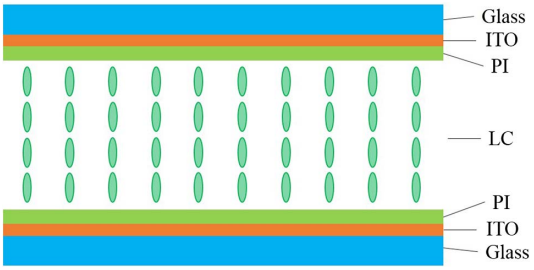

Fig. 1. Structure of VAN cell.

The VAN LC cell used in this Letter was provided by Hebei Jiya Electronics Co., Ltd., and its structure is shown in Fig. 1. When no voltage is applied, the LC molecules are arranged vertically on the substrate.

The experimental device for evaluating image sticking by the capacitance voltage method is shown in Fig. 2. The capacitance value of the LC cell is measured using a precision inductance-capacitance-resistance (LCR) meter E4980A, and the temperature of the LC cell controlled by the precision hot stage is 28°C.

The *C*-*U* curve of the VAN cell under 1 kHz was measured, as shown in Fig. 3. According to the capacitance voltage curve, the relationship between the capacitance slope and voltage is obtained, as shown in Fig. 4. Select the voltage corresponding to the position of the maximum capacitance slope as the AC voltage value of evaluating the RDCV. Here, taking the test result of the 3.85 μm VAN cell as an example, the selected AC voltage is 2.2 V. When the voltage is in the range of 2.0–2.6 V (illustrated in Fig. 3), the capacitance increases linearly. When a DCB is applied to the LC cell at 2.2 V AC voltage, the

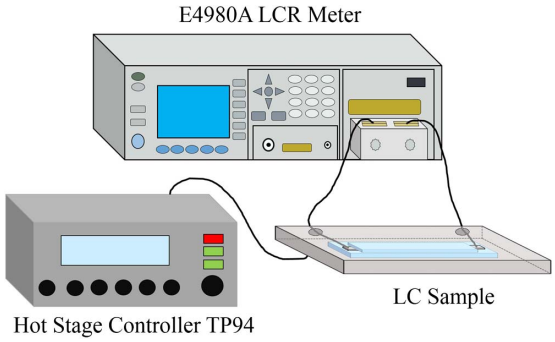

Fig. 2. Experimental device for evaluating image sticking by the capacitance voltage method.

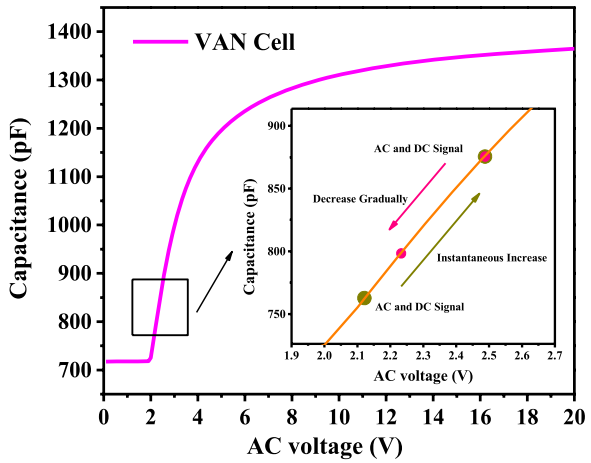

Fig. 3. *C-U* curve and RDCV evaluation principle of FFS1 in the VAN cell.

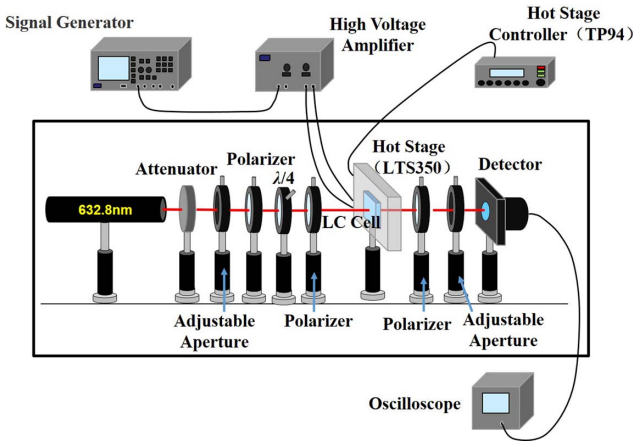

Fig. 5. VAN cell response time measurement setup.

capacitance of the LC cell will increase instantaneously. As the impurity ions in the LC cell gradually accumulate toward the two substrates under the action of DCB, an internal electric field will be formed, which will decrease the effective voltage value on the LC layer, so the capacitance value of the LC cell will gradually decrease. In the experiment, the value of the VAN cell capacitance changing with time is recorded, and the RDCV is calculated by the capacitance voltage relationship when DCB is not added, that is, the voltage value corresponding to the 0 s after adding DCB is subtracted from the voltage value corresponding to the capacitance value at each time point, and the variation curve of RDCV with time is obtained.

Response time is also an important parameter to evaluate the performance of the display. The shorter the response time of the LC is, the less likely the image sticking phenomenon will occur. The response time of pure FFS1 LC and γ-Fe_2O_3 nanoparticles-doped LC mixture was also measured in this Letter. The setup for measuring the response time of the VAN cell is shown in Fig. 5. The laser with a wavelength of 632.8 nm becomes circularly polarized light after passing through the $\lambda/4$ wave plate and becomes linearly polarized light after passing through the polarizer. The angle between the direction of polarization and detection is 90°, and the temperature of the LC cell is controlled at 28°C. The combined waveform of the 0 V DC and 1 kHz AC square wave is generated by the signal generator, and the total period is 2 s, which is amplified by the high-voltage amplifier to supply voltage to the LC cell. When the voltage is greater than the threshold voltage of the LC, the LC molecules rotate, then the light intensity changes, and the detector collects the signal and displays it by the oscilloscope, where the response time can be obtained.

At 2.2 V AC voltage, the relationship between the capacitance and time of the 3.85 μm VAN cell perfused with pure FFS1 LC at 0.4 V, 0.6 V, and 0.8 V DCB was measured, and the variation curve of RDCV with time was calculated from the *C-U* curve, as shown in Fig. 6. After the application of DCB, the RDCV increases instantly and tends to be stable with time; the larger the DCB is, the greater the RDCV value is.

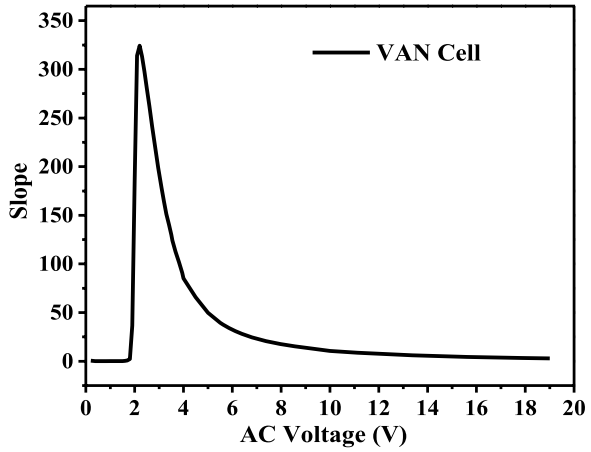

Fig. 4. Curve of capacitance slope variation with AC voltage in negative LC FFS1 in VAN cell.

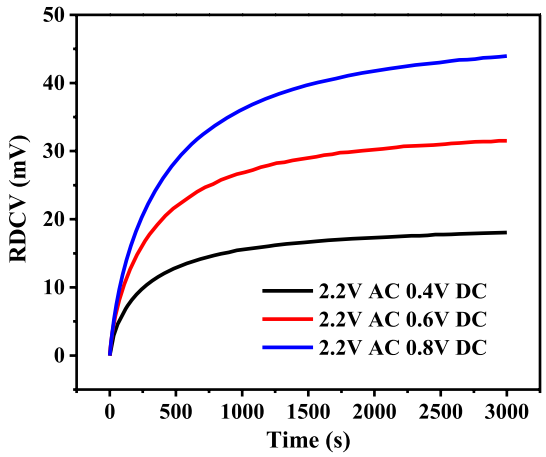

Fig. 6. Curve of RDCV in VAN cell varies with time when DCB is 0.4 V, 0.6 V, and 0.8 V, respectively.

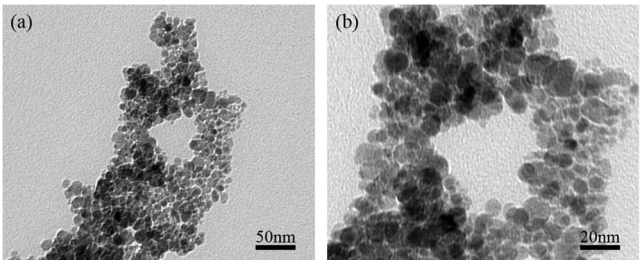

Fig. 7. TEM image of γ-Fe_2O_3 nanoparticles: (a) 43,000 times, (b) 97,000 times.

The microscopic morphology of γ-Fe_2O_3 nanoparticles in the transmission electron microscope (TEM) is shown in Fig. 7: Fig. 7(a) is a 43,000 times magnified image, Fig. 7(b) is a 97,000 times magnified image, and the shape of nanoparticles is basically spherical.

Seven concentrations of γ-Fe_2O_3 nanoparticles and FFS1 LC mixtures were configured in the experiment, where the concentrations were 0.017 wt.%, 0.034 wt.%, 0.051 wt.%, 0.068 wt.%, 0.136 wt.%, 0.204 wt.%, and 0.272 wt.%, respectively. The pure FFS1 LC and seven LC mixtures were separately injected into the PAN cell and the VAN cell under the same experimental environment. Using POM to observe the PAN cell, 300 times magnified images of pure LC and the LC mixture of different concentrations of nanoparticles were obtained, as shown in Fig. 8. Compared with the LC materials of undoped nanoparticles, no obvious anomalies were observed after doping, indicating that the nanoparticles did not distinctly affect the alignment of the LC molecules. The measured physical properties of the LC mixtures are as shown in Table 1. After the doping, the clearing point temperature of the LC materials slightly increases, and the threshold voltage slightly decreases.

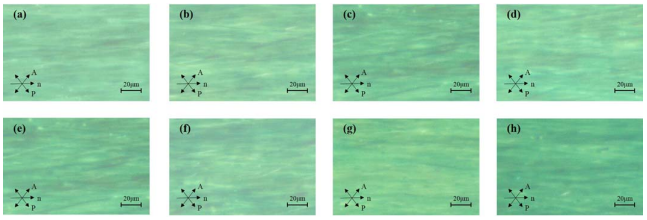

Fig. 8. POM image of PAN cell undoped and doped with different concentrations of γ-Fe_2O_3 nanoparticles. (a) Undoped, (b) 0.017 wt.%, (c) 0.034 wt.%, (d) 0.051 wt.%, (e) 0.068 wt.%, (f) 0.136 wt.%, (g) 0.204 wt.%, and (h) 0.272 wt.%. A and P represent the perpendicular analyzer and polarizer, respectively, and n represents the rubbing direction of PI.

The experimental results show that the SRDCV of the 3.85 μm VAN cell changes with the doping concentration of nanoparticles under different DCBs. As shown in Fig. 9, while the applied AC voltage was 2.2 V, DCBs were 0.4 V, 0.6 V, and 0.8 V. The SRDCV decreases first and then increases with the increase of doping concentration. The SRDCV corresponding to the concentration of 0.034 wt.% is lower than that of other doping concentrations, about 70% of the undoped samples, which indicates γ-Fe_2O_3 nanoparticles can effectively reduce the impurity ions and obtain a lower SRDCV value, and the value of SRDCV is the corresponding RDCV value at 3000 s.

In addition, the variation of SRDCV of the 11.5 μm VAN cell with the doping concentration of nanoparticles was also measured, as shown in Fig. 10, where the applied

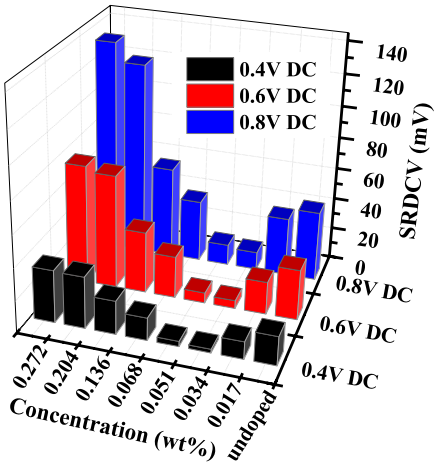

Fig. 9. Relationship between SRDCV and doping concentration in the 3.85 μm VAN cell under 0.4 V, 0.6 V, and 0.8 V DCB.

Table 1. Negative LC Parameters with Undoped and Doped γ-Fe_2O_3 Nanoparticles

Samples	Clearing Point (°C)	U_{th} (V)	$\Delta\varepsilon$	k_{33} (pN)	γ_1 (mPa · s)
Undoped FFS1	78.7	1.988	−4.212	14.93	27.71
FFS1 + 0.017 wt.% γ-Fe_2O_3	78.8	1.968	−3.994	13.88	25.65
FFS1 + 0.034 wt.% γ-Fe_2O_3	78.8	1.975	−4.043	14.15	26.19
FFS1 + 0.051 wt.% γ-Fe_2O_3	79.0	1.974	−4.249	14.85	27.53
FFS1 + 0.068 wt.% γ-Fe_2O_3	79.1	1.971	−4.044	14.08	26.31
FFS1 + 0.136 wt.% γ-Fe_2O_3	80.6	1.959	−4.322	14.87	27.79
FFS1 + 0.204 wt.% γ-Fe_2O_3	80.8	1.951	−4.388	14.97	27.99
FFS1 + 0.272 wt.% γ-Fe_2O_3	82.2	1.933	−4.493	15.06	28.18

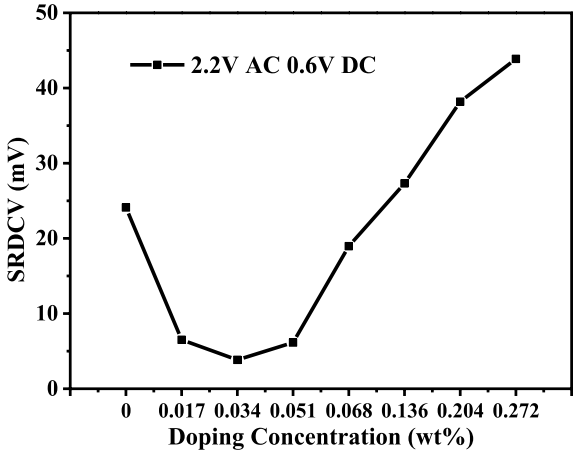

Fig. 10. Relationship between SRDCV and doping concentration in the 11.5 μm VAN cell under 0.6 V DCB.

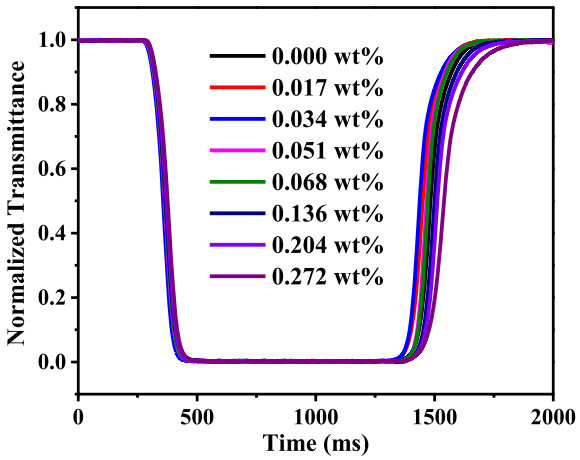

Fig. 11. Decay and rise times at different doping concentrations in the 11.5 μm VAN cell.

AC voltage was 2.2 V, and the DCB was 0.6 V. The SRDCV decreases first and then increases with the increase of the doping concentration, which is the same as the change trend in the 3.85 μm VAN cell. The SRDCV measured at the doping concentrations of 0.017 wt.%, 0.034 wt.%, 0.051 wt.%, and 0.068 wt.% is lower than that of the pure LC material, and the SRDCV value is more than 80% lower than that of the pure FFS1 LC at the doping concentration of 0.034 wt.%. It is shown that the image sticking of the VAN cell can be greatly improved by adding proper concentrations of γ-Fe_2O_3 nanoparticles into negative LC material FFS1.

In summary, the γ-Fe_2O_3 nanoparticles in the VAN cell can adsorb the freely moving ionic impurities in FFS1 LC

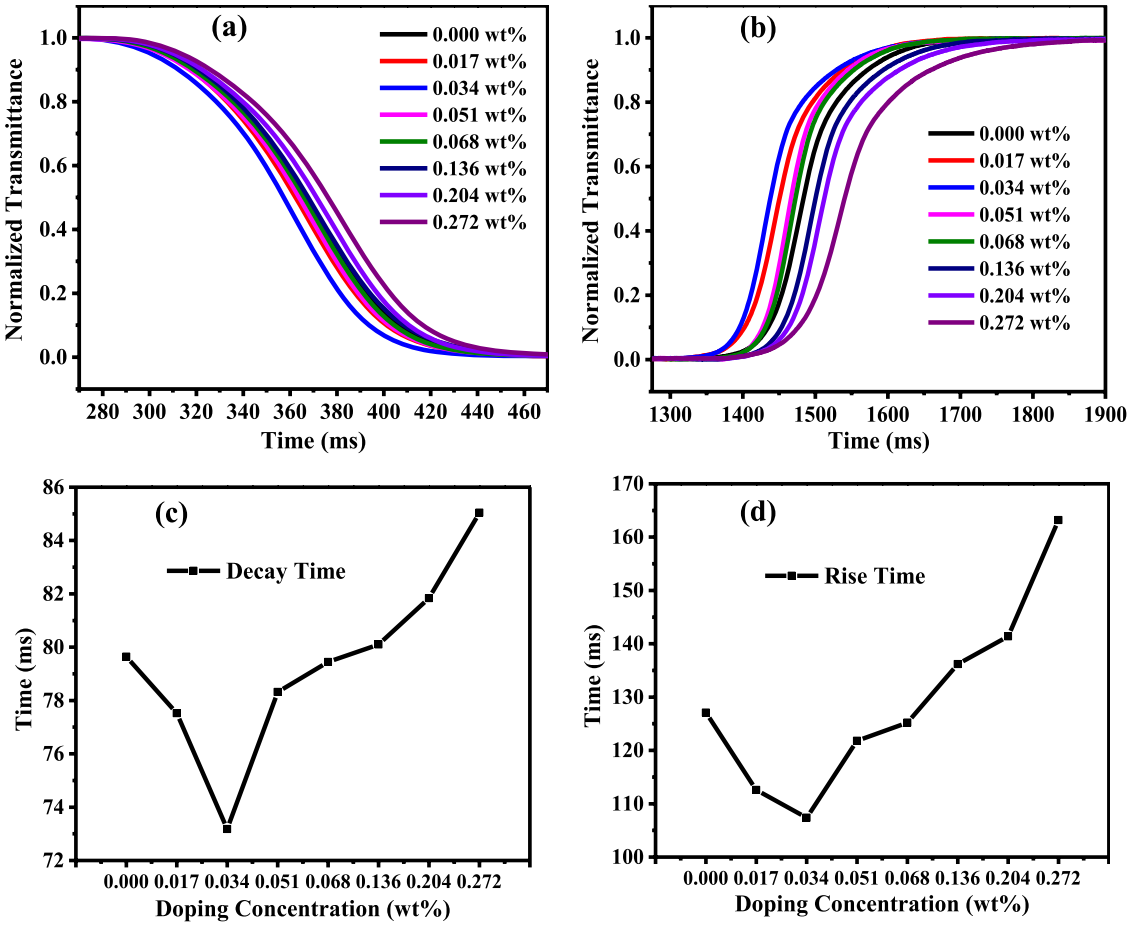

Fig. 12. Relationship between doping concentration and response time. (a) Normalized transmittance and decay time. (b) Normalized transmittance and rise time. (c) Decay time and doping concentration. (d) Rise time and doping concentration.

material, thereby reducing the SRDCV of the VAN cell, and the adsorption capacity of the nanoparticles has a close relationship with the doping concentration. The impurity ions in the VAN cell show two trends with the increase of the concentration of γ-Fe_2O_3 nanoparticles: when the doping concentration is low, the SRDCV decreases with the increase of the concentration; until the concentration of 0.034 wt.%, SRDCV decreases to the lowest value. At this concentration, the nanoparticles can adsorb a large number of ion impurities in the LC layer, and a very small amount of impurity ions accumulate in the upper and lower alignment layer positions under the action of DCB, which leads to the decrease of SRDCV. When the doping concentration continues to increase, the cluster aggregation phenomenon of γ-Fe_2O_3 nanoparticles may occur, as mentioned in Ref. [19], which reduces the adsorption area of the surface and weakens the ability to adsorb ions, where the number of free ions in the LC layer increases relatively, and the SRDCV increases.

The experiment tested the change of the response time of the 11.5 μm VAN cell, as shown in Fig. 11, where the doping of γ-Fe_2O_3 nanoparticles also had a certain effect on the response time. In order to make the test results clearer, Figs. 12(a) and 12(b) show the amplification diagrams of the decay and rise time, respectively, where the decay and rise times correspond to the process of removing voltage and adding voltage, respectively. Figures 12(c) and 12(d) show the relationship between the decay time and the rise time with the doping concentration, respectively. It can be seen from the figure that the trend of response time with concentration is the same as that of SRDCV with concentration; that is, it decreases first and then increases with the increase of concentration, and the response time is the shortest at the concentration of 0.034 wt.%. Compared with the undoped case, the decay time can be increased by up to 8.11%, and the rise time can be increased by up to 15.49%.

In this Letter, the effect of nanoparticles doping negative LC on SRDCV and response time is measured, and then the image sticking problem in the VAN cell is analyzed. It is found that the impurity ions decrease firstly and then increase with the increase of the doping concentration of nanoparticles. When the doping concentration is 0.034 wt.%, a large number of impurity ions are adsorbed to reduce the SRDCV by more than 70%, the decay time by 8.11%, and the rise time by 15.49%. The experimental results show that γ-Fe_2O_3 nanoparticles can effectively improve the image sticking of the VAN LC display mode, which has certain guiding significance for the improvement of image sticking in other LCD modes.

This work was supported by the National Natural Science Foundation of China (NSFC) (Nos. 11374087 and 11504080), the Natural Science Foundation of Hebei Province of China (Nos. A2019202235 and A2017202004), and the Key Subject Construction Project of Hebei Province University.

References

1. T. Kim, J. H. Lee, T. H. Yoon, and S. W. Choi, Opt. Express **20**, 15522 (2012).
2. A. B. Watson, SID Int. Symp. Dig. Tech. Pap. **37**, 1312 (2006).
3. T. R. Lee, J. H. Kim, S. H. Lee, M. C. Jun, and H. K. Baik, Liq. Cryst. **44**, 738 (2017).
4. Z. Diao, L. Kong, J. Yan, J. Guo, X. Liu, L. Xuan, and L. Yu, Chin. Opt. Lett. **17**, 012301 (2019).
5. C. Chang, Y. Qi, J. Wu, J. Xia, and S. Nie, Chin. Opt. Lett. **16**, 100901 (2018).
6. V. Tkachenko, G. Abbate, A. Marino, E. Santamato, N. Bennis, X. Quintana, and J. M. Otón, in *International Conference on Advanced Optoelectronics & Lasers* (2008), p. 33.
7. B. W. Park, J. W. Kim, S. W. Oh, J. W. Huh, and T. H. Yoon, SID Int. Symp. Dig. Tech. Pap. **45**, 1473 (2014).
8. D. Xu, F. Peng, H. Chen, J. Yuan, S. T. Wu, M. C. Li, S. L. Lee, and W. C. Tsai, J. Appl. Phys. **116**, 193102 (2014).
9. P. L. Chen and S. H. Chen, Liq. Cryst. **27**, 965 (2000).
10. C. S. Woo, S. H. Hong, D. S. Oh, M. S. Chung, H. S. Kim, Y. Nam, J. Y. Lee, M. C. Jun, and I. B. Kang, SID Int. Symp. Dig. Tech. Pap. **47**, 858 (2016).
11. M. Mizusaki, T. Miyashita, and T. Uchida, J. Appl. Phys. **108**, 104903 (2010).
12. M. Mizusaki, Y. Nakanishi, S. Enomoto, and Y. Hara, Liq. Cryst. **43**, 1208 (2016).
13. K. T. Huang, A. Chao, and C. H. Yu, SID Int. Symp. Dig. Tech. Pap. **38**, 665 (2007).
14. M. Mizusaki, T. Miyashita, T. Uchida, Y. Yamada, Y. Ishii, and S. Mizushima, J. Appl. Phys. **102**, 014904 (2007).
15. K. T. Huang, Y. W. Hung, R. X. Fang, Y. T. Chao, C. Lee, S. C. Lin, C. H. Yu, C. Kao, and T. S. Jen, SID Int. Symp. Dig. Tech. Pap. **49**, 1711 (2018).
16. H. J. Park, L. Lai, S. H. Lin, and K. H. Yang, SID Int. Symp. Dig. Tech. Pap. **34**, 204 (2003).
17. T. Sasaki, M. Tsumura, Y. Nagae, M. Suzuki, and T. Iwata, Electr. Commun. Jpn. **78**, 79 (1995).
18. D. Xu, F. Peng, H. Chen, J. Yuan, S. T. Wu, M. C. Li, S. L. Lee, and W. C. Tsai, SID Int. Symp. Dig. Tech. Pap. **46**, 739 (2015).
19. Y. Garbovskiy, Appl. Phys. Lett. **110**, 041103 (2017).
20. Y. Yasuda, H. Naito, M. Okuda, and A. Sugimura, Mol. Cryst. Liq. Cryst. **263**, 559 (1995).
21. L. Gao, Y. Y. Dai, T. Li, Z. Tang, X. Zhao, Z. Li, X. Meng, Z. He, J. Li, M. Cai, X. Wang, J. Zhu, X. Xing, and W. Ye, Nanomaterials **8**, 8110911 (2018).
22. K. Tsutsui, T. Sakai, K. Goto, K. Sawahata, M. Ishikawa, and H. Fukuro, SID Int. Symp. Dig. Tech. Pap. **34**, 1166 (2003).
23. S. M. Seen, M. S. Kim, and S. H. Lee, Jpn. J. Appl. Phys. **49**, 050208 (2010).
24. W. Ye, R. Yuan, Y. Dai, L. Gao, Z. Pang, J. Zhu, X. Meng, Z. He, J. Li, M. Cai, X. Wang, and H. Xing, Nanomaterials **8**, 8010005 (2018).
25. M. Mizusaki and Y. Nakanishi, Liq. Cryst. **43**, 704 (2016).
26. M. Mizusaki, S. Enomoto, Y. Hara, H. Kikuchi, and Y. Yamada, J. Appl. Phys. **113**, 174502 (2013).
27. S. Yuan, L. Wang, F. Liu, F. Zhou, M. Li, H. Xu, Y. Nie, J. Nan, and H. Zeng, Chin. Opt. Lett. **17**, 032601 (2019).
28. I. Dierking, G. Scalia, and P. Morales, J. Appl. Phys. **97**, 044309 (2005).
29. W. K. Lee, J. H. Choi, H. J. Na, J. H. Lim, J. M. Han, J. Y. Hwang, and D. S. Seo, Opt. Lett. **34**, 3653 (2009).
30. B. J. Liang, D. G. Liu, W. L. Tsai, P. F. Hsu, B. J. Jin, M. L. Hsiau, and R. F. Louh, IEEE Trans. Device. Mat. Re. **14**, 35 (2014).

31. T. Zhang, X. Meng, Z. He, Y. Lin, X. Liu, D. Li, J. Li, and X. Qiu, Nanomaterials **7**, 7080220 (2017).
32. B. Wen, J. Li, Y. Lin, X. Liu, J. Fu, H. Miao, and Q. Zhang, Mater. Chem. Phys. **128**, 35 (2011).
33. Y. Chen, Q. Chen, H. Mao, T. Zhang, X. Qiu, Y. Lin, and J. Li, Nanomater. Nanotechno. **7**, 1 (2017).
34. W. Ye, Z. Li, R. Yuan, P. Zhang, T. Sun, M. Cai, X. Wang, J. Zhu, Y. Sun, and H. Xing, Liq. Cryst. **46**, 349 (2019).